

OPEN ACCESS

Polyketones as Host Materials for Solid Polymer Electrolytes

To cite this article: Therese Eriksson *et al* 2020 *J. Electrochem. Soc.* **167** 070537

View the [article online](#) for updates and enhancements.



PRIME™
PACIFIC RIM MEETING
ON ELECTROCHEMICAL
AND SOLID STATE SCIENCE
2020

Abstract Submission
DEADLINE EXTENDED:
May 1, 2020

Honolulu, HI | October 4-9, 2020







Polyketones as Host Materials for Solid Polymer Electrolytes

Therese Eriksson,¹ Amber Mace,¹ Yumehiro Manabe,² Masahiro Yoshizawa-Fujita,³ Yasuhide Inokuma,² Daniel Brandell,¹ and Jonas Mindemark^{1,z}

¹Department of Chemistry—Ångström Laboratory, Uppsala University, Uppsala SE-751 21, Sweden

²Division of Applied Chemistry, Faculty of Engineering, Hokkaido University, Sapporo 060-8628, Japan

³Department of Materials and Life Sciences, Sophia University, Chiyoda-ku, Tokyo 102-8554, Japan

While solid polymer electrolytes (SPEs) have great potential for use in future lithium-based batteries, they do, however, not display conductivity at a sufficient level as compared to liquid electrolytes. To reach the needed requirements of lithium batteries it is therefore necessary to explore new materials classes to serve as novel polymer hosts. In this work, SPEs based on the polyketone poly(3,3-dimethylpentane-2,4-dione) were investigated. Polyketones are structurally similar to several polycarbonate and polyester SPE hosts investigated before but have, due to the lack of additional oxygen atoms in the coordinating motif, even more electron-withdrawing carbonyl groups and could therefore display better properties for coordination to the salt cation. In electrolyte compositions comprising 25–40 wt% LiTFSI salt, it was observed that this polyketone indeed conducts lithium ions with a high cation transference number, but that the ionic conductivity is limited by the semi-crystallinity of the polymer matrix. The crystallinity decreases with increasing salt content, and a fully amorphous SPE can be produced at 40 wt% salt, accompanied by an ionic conductivity of $3 \times 10^{-7} \text{ S cm}^{-1}$ at 32 °C. This opens up for further exploration of polyketone systems for SPE-based batteries.

© 2020 The Author(s). Published on behalf of The Electrochemical Society by IOP Publishing Limited. This is an open access article distributed under the terms of the Creative Commons Attribution Non-Commercial No Derivatives 4.0 License (CC BY-NC-ND, <http://creativecommons.org/licenses/by-nc-nd/4.0/>), which permits non-commercial reuse, distribution, and reproduction in any medium, provided the original work is not changed in any way and is properly cited. For permission for commercial reuse, please email: oa@electrochem.org. [DOI: 10.1149/1945-7111/ab7981]



Manuscript submitted December 30, 2019; revised manuscript received February 8, 2020. Published March 13, 2020. *This paper is part of the JES Focus Issue on Challenges in Novel Electrolytes, Organic Materials, and Innovative Chemistries for Batteries in Honor of Michel Armand.*

Since the ground-breaking efforts of Michel Armand in the 1970s, it has been clear that solid polymer electrolytes (SPEs) are a good strategy to increase the safety of lithium ion batteries.^{1,2} While continuing his work on SPEs (where a salt is dissolved in a solvent-free polymer matrix), Prof. Armand was also part of the discovery that the ion conduction mainly occurs in the amorphous phases of the poly(ethylene oxide) (PEO) matrix.³ This finding means that crystallinity is often considered as being a negative property of SPEs, which will decrease the ionic conductivity of the electrolyte. This is something that researchers are still struggling with to this day. Even though semi-crystalline PEO-based SPEs have been extensively studied since their discovery in the 1970s, the low ionic conductivity is still a serious problem for these systems.^{4,5} It is therefore important to explore new categories of polymers with ion-coordinating capabilities that can dissolve lithium salts and provide efficient conductive pathways for Li⁺ ions.

As stated, one issue with the commonly used host material PEO is the high degree of crystallinity of PEO itself and PEO-based SPEs.⁶ As the conduction of ions occurs in the amorphous regions of the SPE, the crystalline regions do not contribute to the conductivity and will therefore lower the overall ionic conductivity of the electrolyte.^{3,4} Many batteries based on SPEs are therefore operated at elevated temperatures to decrease the degree of crystallinity as the crystallites melt.⁵ The crystalline regions do, however, contribute to the mechanical stability of the materials, which is also an important aspect for functional SPEs.^{5,7} PEO-based and other semi-crystalline electrolytes thereby often display a trade-off between conductivity and mechanical stability, which is largely temperature-controlled. There are, however, ways to reduce or remove the degree of crystallinity in PEO-based electrolytes, without sacrificing the mechanical properties. This can, for example, be achieved by UV-induced cross-linking. It has previously been shown that cross-linked PEO-based electrolytes show both a reduced degree of crystallinity, while also improving the mechanical properties.⁸ Another approach is inorganic additives or composite electrolytes. With the addition of lithium-conducting ceramic particles both the

mechanical properties as well as the ionic conductivity can be significantly improved.^{9–11}

In contrast to the polyether PEO, this work explores a polyketone: poly(3,3-dimethylpentane-2,4-dione). This category of polymers is basically unstudied previously for these applications, but has structural similarity with the more thoroughly investigated polyesters and polycarbonates.⁴ It is therefore reasonable to believe that polyketones constitute a viable option for use as SPE host materials in lithium-based batteries based on the coordinating motif. The lithium-coordinating carbonyl group of the polyketone is similar to that of these other macromolecular solvents, and where preferential Li⁺–carbonyl oxygen coordination has been found.¹² Furthermore, the physical properties of the polyketone material used in this study is similar to that of several polyethers or polyesters in the sense that it has a relatively high degree of crystallinity.

Polyketones constitute a diverse class of polymers which, in their simplest form, can be synthesized from ethylene and carbon monoxide, thereby producing a semi-crystalline polymer with low solubility and relatively high melting point.^{13,14} While polyketones have not yet entered the realm of SPEs for lithium-ion batteries, they have been researched for use as anion-exchange membranes or organic electrodes in energy storage applications,^{13,15–17} and there displayed good thermal and chemical stability.

Since the polyketone is highly similar to some of the most used and researched polymer electrolyte materials, it is relevant to investigate if this polymer has the ability to conduct lithium ions, and the mechanism behind the ion conduction. This work shows that it indeed does have the ability to coordinate and conduct lithium ions, but that the degree of crystallinity has a high impact on the ionic conductivity as well as the conduction mechanism. This can, however, be overcome by the addition of salt.

Experimental

Materials.—Poly(3,3-dimethylpentane-2,4-dione) was synthesized in accordance with previous work¹⁸ and was vacuum-dried at 40 °C overnight before use. The polymer had a degree of polymerization of 5.1, with a polydispersity index of 1.24. Commercial poly(ethylene oxide) (PEO; M_v 2000000, Sigma-Aldrich) and poly(ε-caprolactone) (PCL; Capa 6500, mean molecular weight 50 000,

^zE-mail: jonas.mindemark@kemi.uu.se

Perstorp) was used as reference materials. LiTFSI (BASF) was vacuum-dried at 120 °C for 24 h before use. All chemicals were stored in an argon-filled glovebox after drying.

Fabrication of polymer electrolyte films.—The vacuum-dried polyketone was mixed and ground with a mortar and pestle with 25 wt%, 32 wt% or 40 wt% LiTFSI until homogenous. This corresponds to an O:Li⁺ ratio of approximately 14, 10 and 7, respectively. The mixture was hot-pressed at 2 MPa and 100 °C for 1 h between two PTFE sheets. For comparison, PCL and PEO films were fabricated with the same procedure with a O:Li ratio of 10. The polyketone films with 25–32 wt% LiTFSI were brittle, whilst films with 40 wt% salt were relatively soft and sticky. The preparation of the films was done in an argon-filled glove box.

Characterization.—To investigate the thermal stability, thermogravimetric analysis (TGA) was performed on the pure polymer using a TA instruments TGA Q500 with a heating rate of 5 °C/min up to 400 °C in a nitrogen atmosphere. Differential scanning calorimetry (DSC) measurements were done on the pure polymer as well as the salt-containing films of the polyketone, PCL and PEO using a TA Q2000 instrument to detect the glass transition temperature, melting temperature and crystallinity. The samples were rapidly cooled to –80 °C, then heated at 10 °C/min to 140 °C, cooled at 5 °C/min to –80 °C and lastly heated to 180 °C at 10 °C/min. FT-IR measurements were performed with a PerkinElmer Spectrum One FT-IR spectrometer. To determine the total ionic conductivity of the films, electrochemical impedance spectroscopy (EIS) was performed on a Schlumberger SI 1260 instrument. The polymer electrolyte films were sandwiched between two stainless steel blocking electrodes in a CR2025 coin cell or, when the mechanical properties were insufficient, a Swagelok cell setup. The measurements were done in the frequency range of 1 Hz to 10 MHz with an amplitude of 10–50 mV during heating from 30 °C up to 105 °C and during cooling back down to 30 °C. The data were fitted to a Debye equivalent circuit to obtain the electrolyte resistance, from which the ionic conductivity was calculated. The transference number was measured and calculated according to the Bruce–Vincent method¹⁹ in symmetrical lithium metal (15 mm diameter) cells at 80 °C. The measurement was conducted using a BioLogic SP-240 Potentiostat. The impedance measurement was done between 100 mHz and 5 MHz (amplitude 10 mV and a bias of 0 V or 10 mV), before and after applying a polarization bias of 10 mV, respectively. The bulk and interface resistances were obtained by fitting an equivalent circuit, and the initial current was calculated from the applied potential and the total resistance of the cell.

Density functional theory calculations.—Density functional theory (DFT) cluster calculations were carried out to model the vibrational shift of the carbonyl group when coordinated with Li⁺ as observed in FT-IR experiments. To model this, frequency calculations were performed on (1) a single monomer and (2) two monomers in the presence of Li⁺ and TFSI. The calculations were performed with the Gaussian 16 software package²⁰ at the B3LYP-D3/6–311++G level of theory, where the ground state molecular structures were fully optimized and verified by absence of any imaginary frequencies.

Results and Discussion

The polymer chosen for this study is a polyketone with the structure shown in Fig. 1. Its structure is characterized by the alternating 1,3- and 1,4-diketones sequence, which should allow for chelation of cations. The polyketone was synthesized from a bis(enol silyl ether) derivative of 3,3-dimethylpentane-2,4-dione by a silver (I) oxide-mediated oxidative homocoupling reaction in 64% yield as a colorless solid.¹⁴

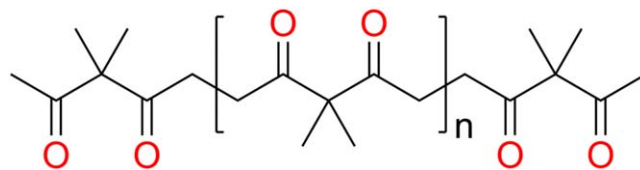


Figure 1. Chemical structure of the poly(3,3-dimethylpentane-2,4-dione) polyketone used in this work.

Thermal analysis.—Many polymer electrolytes are prepared through solvent casting, where a film is produced by dissolving a polymer and a salt in a suitable solvent followed by drying. The polyketone used in this study, however, is not soluble in a solvent suitable for use with lithium salts and glove box atmosphere. Therefore, the polymer electrolyte films were instead prepared by mixing the dry polyketone and salt, followed by hot-pressing. To use this method, it is necessary to know the melting point and the thermal stability of the polymer. TGA analysis showed that the polymer is stable from room temperature up to around 140 °C, as can be seen in Fig. 2. At 350 °C, the entire sample decomposed. This is somewhat lower than PEO, which starts to decompose at 175 °C,²¹ but still higher than the boiling point of liquid electrolytes.^{22,23} This indicates that any processing or non-destructive measurements of this polymer should be restricted to a maximum of 140 °C.

The glass transition temperature (T_g) and melting point (T_m) for the polyketone with and without salt was determined from the first and second heating cycle in the DSC measurements seen in Fig. 3. The melting peaks are wide, starting at 80 °C for the salt-free polyketone sample and continuing until around 130 °C.

With the information from the DSC measurements at hand, electrolyte samples were prepared by hot-pressing at 100 °C. With the addition of 25–32 wt% LiTFSI, the onset of the melting peak decreases to around 50 °C implying a decrease in crystallite size in the sample. The integrated size of the peak is reduced, also indicating an overall lower degree of crystallinity. In contrast with, *e.g.*, electrolytes based on PEO or poly(ϵ -caprolactone) (PCL), no clear transition to the amorphous state is observed, which is likely to also affect the temperature profile of the ionic conductivity. During the second heating step, this melting peak disappears for these

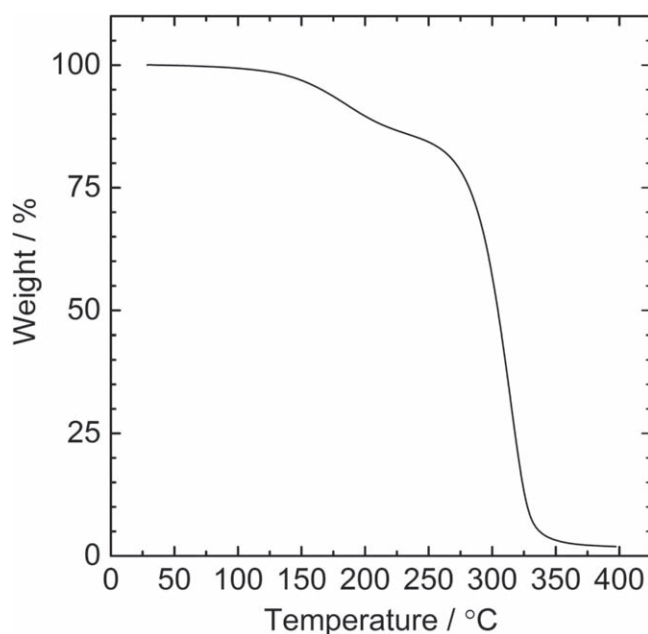


Figure 2. Thermogravimetric analysis of the polymer without salt from room temperature up to 400 °C.

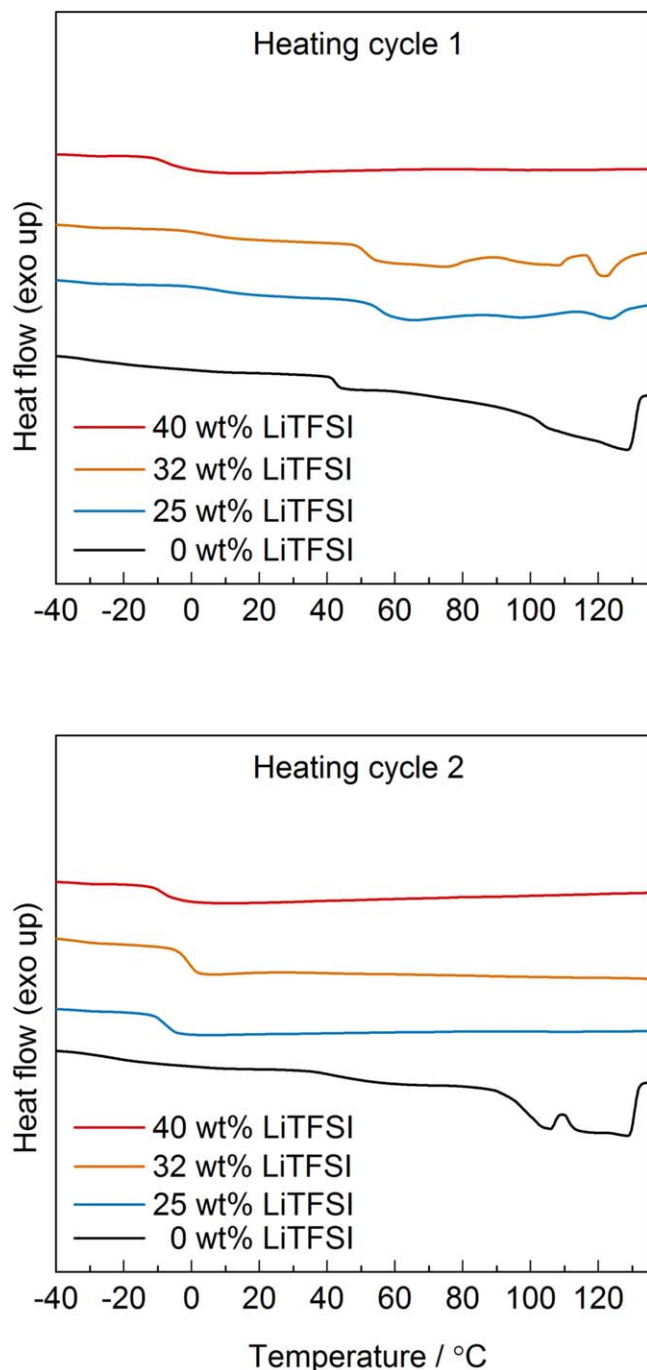


Figure 3. DSC scans for the poly(3,3-dimethylpentane-2,4-dione) without LiTFSI and with 25, 32 or 40 wt% LiTFSI for heating cycle 1 and 2.

samples as it does not have sufficient time to recrystallize during the cooling step. The degree of crystallinity is, however, expected to return to its original value with time. With 40 wt% LiTFSI, no melting peak can be seen in either of the heating runs, and the polymer electrolyte is therefore considered to be fully amorphous.

The glass transition temperature is found at 41 °C–43 °C for the salt-free sample, which is considered quite high compared to several other polymer electrolyte hosts. For example, PEO has a T_g of around -60 °C^{4,5} and PCL likewise has a T_g of -60 °C.²⁴ It is, however, not a necessity to have a low T_g to have a well-functioning SPE. Polymers such as polyacrylonitrile or poly(ethylene carbonate) (PEC) have been researched as polymer hosts with promising results, while having considerably higher T_g than PEO (80 °C and

9 °C, respectively).^{25,26} With the addition of salt, the T_g is reduced to around -2 °C to -9 °C, close to that of poly(trimethylene carbonate)-based electrolytes.²⁷ This is a notable reduction in T_g , and quite opposite the behavior of several other comparable systems where the T_g instead increases with salt concentration due to the creation of physical cross-links between the polymer chains. Here, the salt obviously has a more plasticizing effect. A similar phenomenon has previously been seen in PEC-based electrolytes with moderate to high salt concentrations.^{26,28} This was explained by an increased rotational mobility due to the reduced intermolecular interactions that comes with the coordination between the carbonyl group and lithium ions, as well as an excess of ions and ion aggregates around the saturated PEC chains.²⁹ In the polyketone electrolytes, however, a reduction in T_g is achieved with lower salt concentrations than for PEC and no continuous decrease with increasing salt content is observed, in contrast to the PEC system. Instead, the reduction in T_g is attributed to the samples' high degree of crystallinity and the difficulty of determining an accurate T_g in this type of sample. As the chains are partially incorporated into the crystallites, their mobility will be restricted, leading to a higher T_g than the one seen in a fully amorphous sample.

Ion coordination.—As mentioned, the lithium ions will preferentially coordinate to the carbonyl oxygens in a polycarbonate-based system, and several studies have previously investigated this coordination using FT-IR.^{12,30–33} What is typically seen is a shift of the carbonyl stretching peak (around 1700 cm^{-1}) to lower wavenumbers as Li^+ coordination occurs. This is, however, not what is seen when the same analysis is done on the polyketone system, as shown in Fig. 4a. Here, the shift goes towards higher wavenumbers. To explain this, the equivalent IR spectra were derived computationally by means of DFT calculations, confirming the shift to higher wavenumbers. The carbonyl stretching peak of a molecule corresponding to the structure of the polyketone ion-coordinating motif (structure seen in Fig. 4b) was compared to the peak of a system where also Li^+ and TFSI ions are added. When coordinating to a lithium ion, the peak becomes shifted towards higher wavenumbers as compared to the non-coordinating molecule, seen in Fig. 4b. The carbonyl groups are situated very close to each other in this polyketone structure, unlike the previously studied polycarbonates,^{30,31} allowing for simultaneous coordination by both carbonyl oxygens in this motif to the same Li^+ ion. This is illustrated in Fig. 4c, where a chelating coordination is seen between the two carbonyl oxygens of the ketone molecule and a Li^+ ion. This leads to different conformational changes as Li^+ is coordinated, as compared to other polymers with carbonyl groups, thereby giving a shift towards higher wavenumbers instead of the previously documented shift to lower wavenumbers. To further confirm this, a spectrum was measured on a ketone system (acetone) that does not share the same chelating motif. As can be seen in Fig. 4d, when LiTFSI is dissolved in acetone, the expected shift of the carbonyl peak towards lower wavenumbers appears. This confirms that the shift to higher wavenumbers seen for the polyketone is an effect of the particular coordinating environment, and not a property of the ketone coordinating moiety itself.

Ionic conductivity and transport.—After confirming Li^+ coordination/solvation by the polyketone host, the ionic conductivity was investigated. A fully amorphous polymer electrolyte will have a more or less bent curve when presented in an Arrhenius plot, representing a Vogel–Fulcher–Tammann (VFT) behavior. Highly crystalline polymer electrolytes will, on the other hand, display a more straight and sharply increasing line below the melting point, and a VFT-type dependence above the melting point.⁴ As the polyketone used in this study is semi-crystalline, the effect of the crystallinity on the ionic conductivity mechanism was investigated by measuring the ionic conductivity during both heating and cooling. During cooling, the degree of crystallinity will be lower than during heating as the recrystallization of polymers is limited by slow

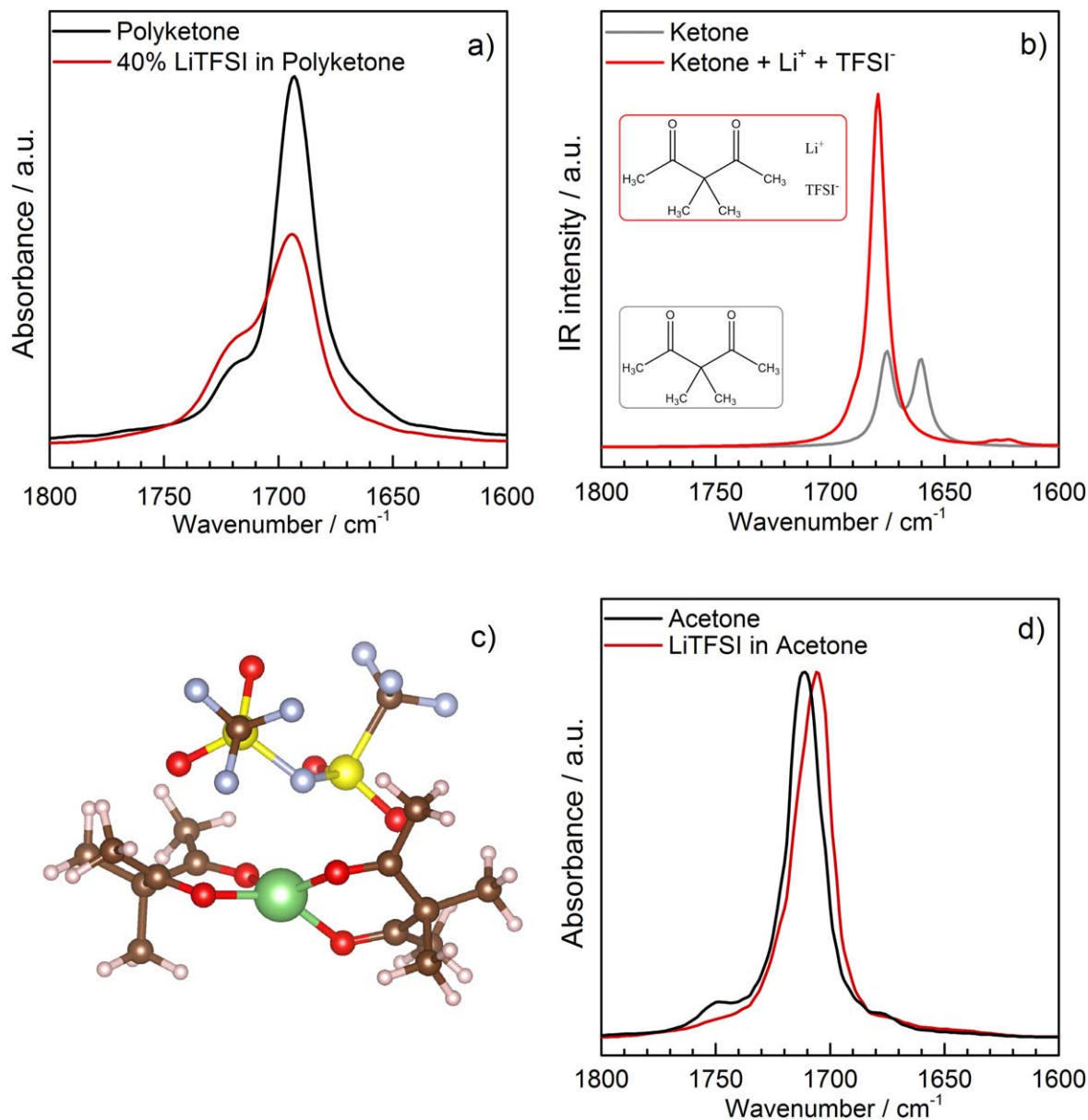


Figure 4. (a) Experimental FT-IR spectra of the polyketone with and without LiTFSI; (b) calculated FT-IR spectra of a diketone mimic by itself and in the presence of a Li⁺ and a TFSI⁻; (c) illustration of coordination between Li⁺ (green) and four oxygens (red) of two ketone molecules; and (d) experimental FT-IR spectra of acetone with or without LiTFSI.

kinetics, and the impact this has on the ionic conductivity may give important clues about the conductivity mechanism.

The total ionic conductivity of samples containing 25 wt%, 32 wt% or 40 wt% LiTFSI is seen in Fig. 5. The behavior of the polyketone with 25 wt% LiTFSI can be compared to that of PEO or PCL, two other semi-crystalline polymers used as SPE hosts.^{3,34} As seen in other studies,^{3,34} a more Arrhenius-type behaviour is seen for the sample below the melting point as a result of the high crystallinity and perhaps associated with the low chain length. Above the melting point, all crystallinity is gone, and a VFT-type behavior is observed. Both PEO and PCL have a melting point of about 60 °C^{4,6,24,34} and a clear transition in conductivity behavior is usually seen at this point. The melting point of this polyketone is not as clearly defined, but is instead spread over a large interval (as seen in Fig. 3). This may be due to inhomogeneities in the crystallite structure, as a similar phenomenon is seen without salt. Melting instead occurs over 50 °C–130 °C as seen in the DSC data, which means that this process is taking place gradually from 50 °C and upwards during the ionic conductivity measurement. Therefore, this

system displays a more diffuse transition during its transition to an amorphous electrolyte.

During the cooling step, however, the transition is much clearer. A drop in conductivity is seen around 70 °C since the polymer is starting to crystallize. As seen in the second heating cycle in the DSC data, the sample will be more amorphous after being heated above the melting point in the timeframe of the experiment. It should be said, however, that the cooling step during the DSC measurement is around 10 times faster than the cooling during the conductivity measurement, meaning that the sample has more time to recrystallize when exploring the conductivity. A similar trend as for the 25 wt% salt sample is seen for the sample containing 32 wt% salt; the drop around the crystallization temperature is, however, not as clear. With the higher amount of conducting amorphous regions in the polymer electrolyte, the total ionic conductivity will be correspondingly higher. This is a clear indication that, as expected, the conduction occurs in the amorphous regions and that the crystallinity reduces the total ionic conductivity.

Since the sample with 40 wt% salt is fully amorphous, no similar effect is seen as for the other samples. This electrolyte can more

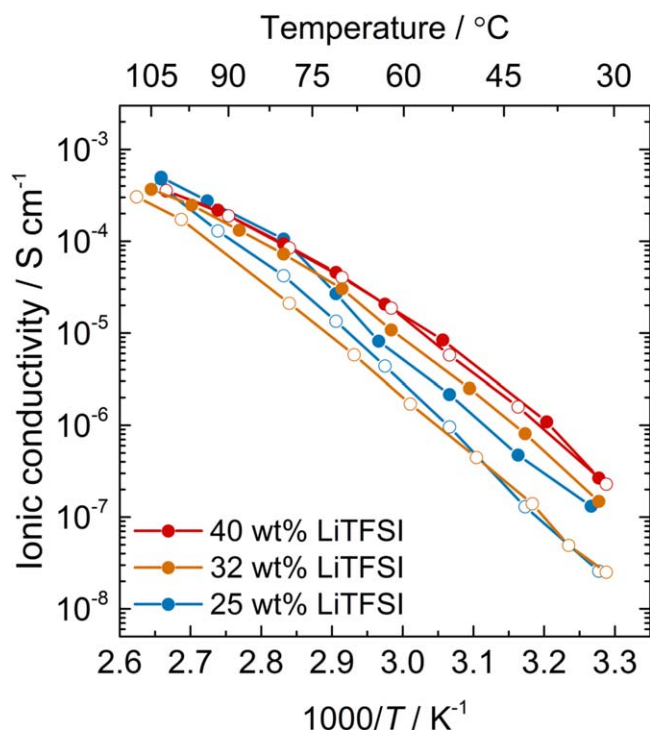


Figure 5. Total ionic conductivity data for the polyketone samples containing 25, 32 or 40 wt% LiTFSI. Open markers indicate measurements during heating and filled markers indicate measurements during cooling.

accurately be compared to fully amorphous SPEs. For example, electrolytes based on poly(trimethylene carbonate) show similar ionic conductivity behavior both in shape of the curve and in terms of absolute values.^{27,35,36} In fact, the polyketone possesses slightly higher conductivity with LiTFSI in comparison. With 40 wt% salt, a VFT-type behavior is observed throughout the investigated temperature interval, and the values are very similar during both heating

and cooling due to the absence of crystallinity. It is interesting to note is that at 80 °C–105 °C, when all samples are fully amorphous, the ionic conductivity is basically the same for the sample containing 40 wt% salt as for the samples with lower salt content. This indicates that it is the degree of crystallinity that primarily limits the total ionic conductivity, and not the amount of charge carriers in the samples containing 25 wt% or 32 wt% salt. As 40 wt% is a relatively high salt content, this may lead to ion pairing and a decrease in the fraction of free charge carriers, which will naturally limit the ionic conductivity.

As a direct comparison of the ionic conductivity, electrolytes based on PEO and the carbonyl-containing PCL were fabricated with an oxygen to lithium ratio corresponding to the polyketone electrolyte with 32 wt% LiTFSI. The ionic conductivities of the three electrolytes are shown in Fig. 6, along with the DSC results for the PEO- and PCL-based electrolytes. At this salt content, the PEO-based electrolyte is fully amorphous and the PCL-based electrolyte shows only a low degree of crystallinity that disappears during the second heating scan. The hysteresis seen in the measured conductivity during heating and cooling in the polyketone sample is therefore not seen in the PCL and PEO samples.

Both the PEO- and the PCL-based electrolyte display a T_g around 30 K lower than the polyketone-based samples, as seen in Fig. 6b. To be able to directly compare the electrolytes, the approach employed by Pesko et al.³⁷ was used, where the ionic conductivity is plotted against a shifted temperature scale taking the T_g into account ($1000/(T - T_g + 50 \text{ K})$). When compensating for the difference in T_g in this way, the ionic conductivity of the polyketone sample still does not reach the level of PEO. It is, however, very much comparable to the ionic conductivity of the PCL electrolyte, when both samples are amorphous. This may be explained by the fact that these two polymers both have a structure containing carbonyl oxygens, unlike PEO, and may therefore have a more similar conduction mechanism.

The cation transference number (*i.e.*, the fraction of ionic current carried by Li^+) was measured for the sample containing 25 wt% LiTFSI at 80 °C according to the method developed by Bruce and Vincent.¹⁹ As the total ionic conductivity does not tell the full story, the transference number (T^+) is an important factor for

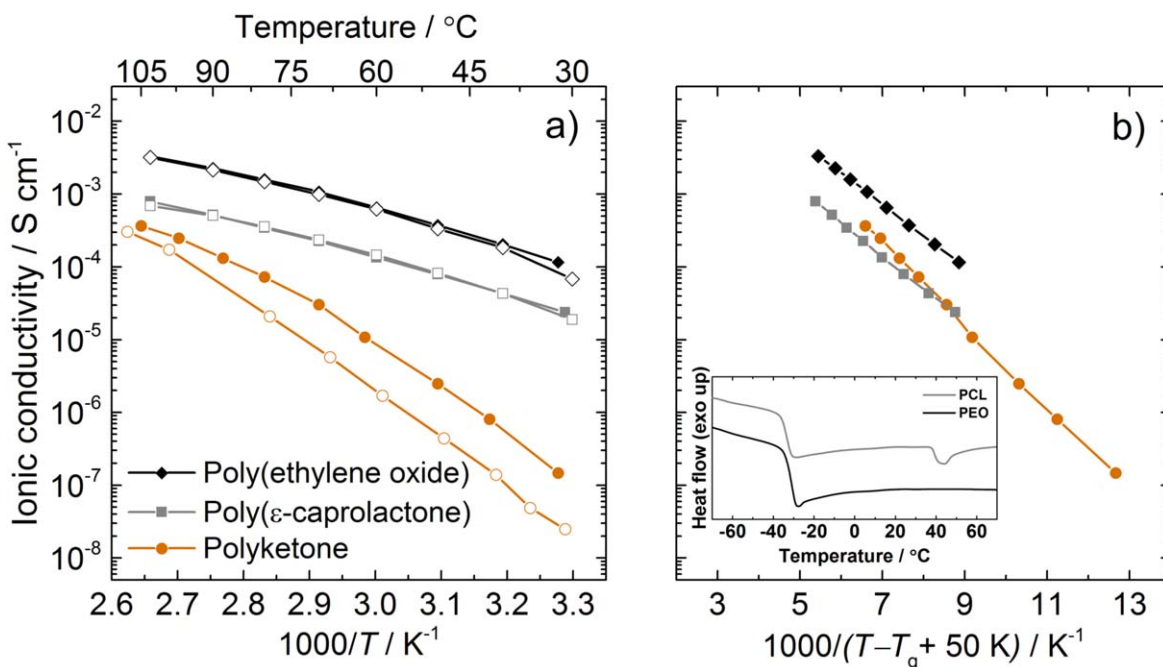


Figure 6. Total ionic conductivity of electrolytes based on the polyketone, PEO and PCL, respectively (all with an O:Li⁺ ratio of 10) plotted against (a) $1000/T$ and (b) the shifted temperature scale $1000/(T - T_g + 50 \text{ K})$. The inset in (b) shows DSC data for the PCL and PEO electrolytes. Open markers indicate measurements during heating and filled markers indicate measurements during cooling.

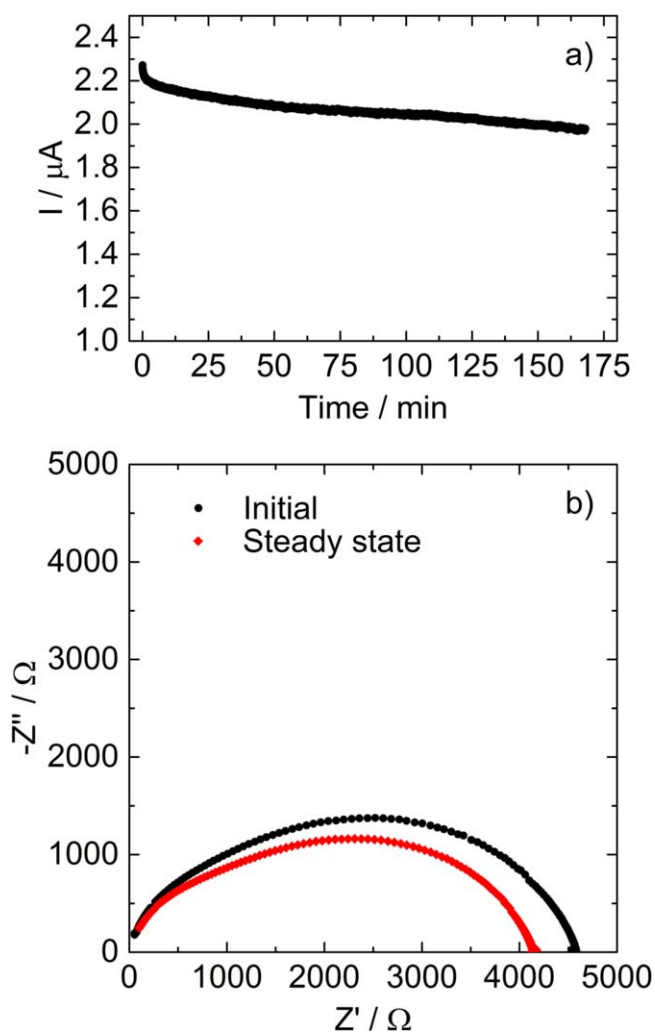


Figure 7. (a) Current relaxation during polarization and (b) Nyquist plot of initial and steady state impedance spectra (before and after polarization).

understanding the conduction mechanism. The current and interfacial resistances derived from the potentiostatic polarization, presented in Fig. 7, was inserted into the Bruce–Vincent equation and a transference number of 0.7 was obtained. Although it is not equal to unity, this value is considerably higher than what has previously been reported for PEO, usually around 0.1–0.2³⁸ and very much in line with what has been seen for other carbonyl-coordinating host materials.^{4,30} This is particularly encouraging for this material, considering that the chelating coordinating motif is expected to bind more strongly to the Li^+ ions than more widely spaced coordinating groups (similar to for example PEO, which also provides chelating structures).⁴ Apparently, the chelating structure formed by these carbonyl groups seems to pose less of a problem for cationic mobility.

Conclusions

In this work, we have explored a novel category of host materials for SPEs: polyketones. This family of compounds displays useful Li^+ -coordinating capabilities and decent ionic conductivity. Electrolytes based on the investigated polyketone electrolyte, poly(3,3-dimethylpentane-2,4-dione), comprising 25 wt% and 32 wt% LiTFSI are semi-crystalline materials and thereby display ionic conductivities that follow the same behavior as many semi-crystalline PEO-based electrolytes, but with a notably higher cation transference number of 0.7. When the salt content is increased to

40 wt%, on the other hand, the polymer is fully amorphous and will behave as such, showing a VFT-type dependence of the ionic conductivity similar to, for example, PTMC-based electrolytes. It seems that, as in many other systems, the degree of crystallinity is a limiting factor for the ionic conductivity, but that this can be overcome by the addition of salt. While this specific polyketone may not be an ideal SPE host material as the molecular weight and degree of crystallinity is not suitable for commercial applications, the demonstration in this study of Li^+ conductivity in a polyketone material may lay the groundwork for this novel class of polymeric host materials.

Acknowledgments

The authors acknowledge funding from the European Research Council (grant number 771777 FUN POLYSTORE) and Sintbat (European Union H2020 research and innovation programme under grant agreement No 685716). The authors further acknowledge STandUP for Energy and the MIRAI collaboration project (supported by STINT). Perstorp AB, Sweden, is also acknowledged for the generous gift of PCL.

ORCID

Therese Eriksson <https://orcid.org/0000-0003-1603-3707>
 Amber Mace <https://orcid.org/0000-0002-0323-0210>
 Masahiro Yoshizawa-Fujita <https://orcid.org/0000-0002-8269-985X>
 Yasuhide Inokuma <https://orcid.org/0000-0001-6558-3356>
 Daniel Brandell <https://orcid.org/0000-0002-8019-2801>
 Jonas Mindemark <https://orcid.org/0000-0002-9862-7375>

References

1. M. Armand, J. M. Chabagno, and M. Duclot, *Second International Meeting on Solid Electrolytes* (St. Andrews, Scotland) (1978).
2. M. B. Armand, J. N. Mundy, and G. K. Shenoy, *Fast Ion Transport in Solids: Electrodes and Electrolytes* (Elsevier North Holland, New York) p. 131 (1979).
3. C. Berthier, W. Gorecki, M. Minier, M. B. Armand, J. M. Chabagno, and P. Rigaud, *Solid State Ionics*, **11**, 91 (1983).
4. J. Mindemark, M. J. Lacey, T. Bowden, and D. Brandell, *Prog. Polym. Sci.*, **81**, 114 (2018).
5. R. C. Agrawal and G. P. Pandey, *J. Phys. D*, **41**, 223001 (2008).
6. B. K. Money and J. Swenson, *Macromolecules*, **46**, 6949 (2013).
7. J.-M. Tarascon and M. Armand, *Nature*, **414**, 359 (2001).
8. M. Falco, C. Simari, C. Ferrara, J. R. Nair, G. Meligrana, F. Bella, I. Nicotera, P. Mustarelli, M. Winter, and C. Gerbaldi, *Langmuir*, **35**, 8210 (2019).
9. J. Lee, T. Howell, M. Rottmayer, J. Boeckl, and H. Huang, *J. Electrochem. Soc.*, **166**, A416 (2019).
10. Z. Xie, Z. Wu, X. An, X. Yue, P. Xiaokaiti, A. Yoshida, A. Abudula, and G. Guan, *J. Membr. Sci.*, **596**, 117739 (2020).
11. G. Piana, F. Bella, F. Geobaldo, G. Meligrana, and C. Gerbaldi, *J. Energy Storage*, **26**, 100947 (2019).
12. R. J. Blint, *J. Electrochem. Soc.*, **142**, 696 (1995).
13. G. Nawn, K. Vezzù, G. Cavinato, G. Pace, and F. Bertasi, *Adv. Funct. Mater.*, **28**, 1706522 (2018).
14. M. Yang, H. Zhao, D. He, C. Hu, H. Chen, and J. Bai, *Materials*, **10**, 741 (2017).
15. J. Geng, J.-P. Bonnet, S. Renault, F. Dolhem, and P. Poizat, *Energy Environ. Sci.*, **3**, 1929 (2010).
16. N. Ataollahi, K. Vezzù, G. Nawn, G. Pace, G. Cavinato, F. Girardi, P. Scardi, V. Di Noto, and R. Di Maggio, *Electrochim. Acta*, **226**, 148 (2017).
17. N. Ataollahi, F. Girardi, E. Cappelletto, K. Vezzù, V. Di Noto, P. Scardi, E. Callone, and R. Di Maggio, *J. Appl. Polym. Sci.*, **134**, 45485 (2017).
18. Y. Manabe, M. Uesaka, T. Yoneda, and Y. Inokuma, *J. Org. Chem.*, **84**, 9957 (2019).
19. J. Evans, C. A. Vincent, and P. G. Bruce, *Polymer*, **28**, 2324 (1987).
20. M. J. Frisch et al., (Gaussian, Inc., Wallingford CT) (2016).
21. R. Tanaka, M. Sakurai, H. Sekiguchi, and M. Inoue, *Electrochim. Acta*, **48**, 2311 (2003).
22. L. Carbone, M. Gobet, J. Peng, M. Devany, B. Scrosati, S. Greenbaum, and J. Hassoun, *ACS Appl. Mater. Interfaces*, **7**, 13859 (2015).
23. E. Knipping, C. Aucher, G. Guirado, and L. Aubouy, *New J. Chem.*, **42**, 4693 (2018).
24. C. P. Fonseca, D. S. Rosa, F. Gaboardi, and S. Neves, *J. Power Sources*, **155**, 381 (2006).
25. M. Forsyth, J. Z. Sun, and D. R. MacFarlane, *Solid State Ionics*, **112**, 161 (1998).
26. Y. Tominaga, V. Nanthana, and D. Tohyama, *Polym. J.*, **44**, 1155 (2012).
27. J. Mindemark, B. Sun, and D. Brandell, *Polym. Chem.*, **6**, 4766 (2015).

28. Y. Tominaga and K. Yamazaki, *Chem. Commun.*, **50**, 4448 (2014).
29. J. Motomatsu, H. Kodama, T. Furukawa, and Y. Tominaga, *Macromol. Chem. Phys.*, **216**, 1660 (2015).
30. B. Sun, J. Mindemark, E. V. Morozov, L. T. Costa, M. Bergman, P. Johansson, Y. Fang, I. Furó, and D. Brandell, *Phys. Chem. Chem. Phys.*, **18**, 9504 (2016).
31. K. Kimura, J. Motomatsu, and Y. Tominaga, *J. Phys. Chem. C*, **120**, 12385 (2016).
32. T. Morioka, K. Ota, and Y. Tominaga, *Polymer*, **84**, 21 (2016).
33. J. Mindemark, L. Imholt, J. Montero, and D. Brandell, *J. Polym. Sci. Part A: Polym. Chem.*, **54**, 2128 (2016).
34. T. Eriksson, J. Mindemark, M. Yue, and D. Brandell, *Electrochim. Acta*, **300**, 489 (2019).
35. M. Smith, *Solid State Ionics*, **140**, 345 (2001).
36. M. M. Silva, S. C. Barros, M. J. Smith, and J. R. MacCallum, *Electrochim. Acta*, **49**, 1887 (2004).
37. D. M. Pesko, Y. Jung, A. L. Hasan, M. A. Webb, G. W. Coates, T. F. Miller, and N. P. Balsara, *Solid State Ionics*, **289**, 118 (2016).
38. O. Buriez, Y. B. Han, J. Hou, J. B. Kerr, J. Qiao, S. E. Sloop, M. Tian, and S. Wang, *J. Power Sources*, **89**, 149 (2000).